MASTER

UCID- 18101

Lawrence Livermore Laboratory

LIMITATIONS TO THE USE OF TWO-DIMENSIONAL THERMAL MODELING OF A NUCLEAR WASTE REPOSITORY

B. W. Davis

January 4, 1979

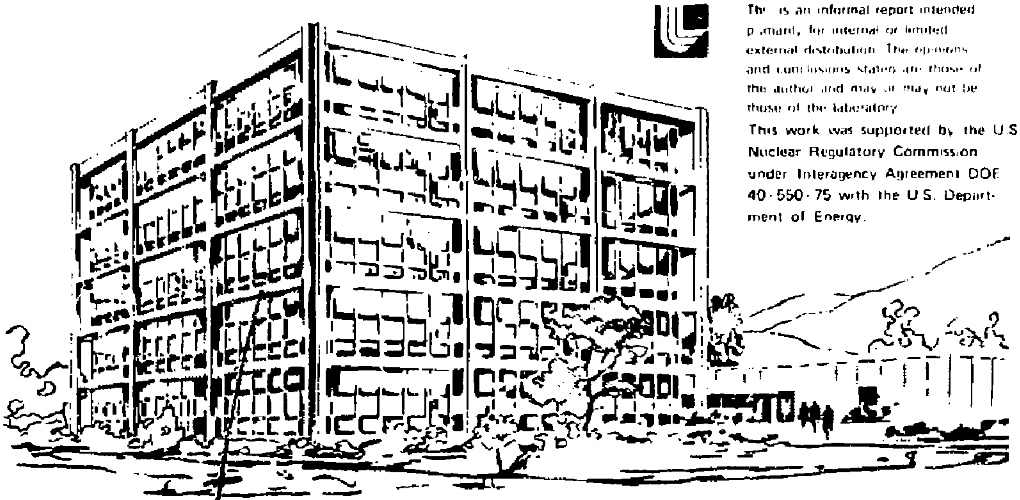

This work was supported by the U.S. Nuclear Regulatory Commission under Interagency Agreement DOE 40-550-75 with the U.S. Department of Energy.

FOREWORD

This report discusses work in thermal modeling under the Nuclear Regulatory Commission program of technical support in the development of nuclear waste management criteria, FIN A0277. The research was performed under the auspices of the U.S. Department of Energy by Lawrence Livermore Laboratory under Contract Number W-7405-ENG-48.

The author acknowledges the support of Dick Martin, who provided initial direction to the thermal analysis effort; Tom Altenbach, who provided necessary TRUMP 2-D results as a basis for evaluating 2-D ADINAT; Henry Cheung, who asked the questions that added directional guidance to the effort; and Dean J. C. Mehrhoff of Northern Arizona University who supported the author's request for a year of leave.

CONTENTS

LIST OF ILLUSTRATIONS

LIST OF TABLES

ABSTRACT

Thermal modeling of a nuclear waste repository is basic to most waste management predictive models. It is important that the modeling techniques accurately determine the time-dependent temperature distribution of the waste emplacement media. Recent modeling studies show that the time-dependent temperature distribution can be accurately modeled in the far-field using a 2-dimensional (2-D) planar numerical model; however, the near-field cannot be modeled accurately enough by either 2-D axisymmetric or 2-D planar numerical models for repositiories in salt. The accuracy limits of 2-D modeling were defined by comparing results from 3-dimensional (3-D) TRUMP modeling with results from both 2-D axisymmetric and 2-D planar. Both TRUMP and ADINAT were employed as modeling tools. Two-dimensional results from the finite element code, ADINAT were compared with 2-D results from the finite difference code, TRUMP; they showed almost perfect correspondence in the far-field. This result adds substantially to confidence in future use of ADINAT and its companion stress code ADINA for thermal stress analysis. ADINAT was found to be somewhat sensitive to time step and mesh aspect ratio.

INTRODUCTION

Approximately 300,000-m^3 of high level nuclear waste exists in temporary surface storage depositories.[1] Most of the waste is military-produced. Commercial power-generating reactors produce about 2200-m^3 of spent fuel waste yearly; one reference reactor operating for one year (RRY*) produces an average of 35-m^3 of spent fuel waste.[1] In June, 1978, there were 68 commercial nuclear reactors operating in the United States[2]; an additional 132 reactors are scheduled to begin power generation in the United States during the 1980's. This projected growth rate intensifies pressure on the Nuclear Regulatory Commission (NRC) to determine methodologies and to develop a knowledge base that will allow them to confidently license other agencies for disposing of waste in more permanent and safe sites.

IMPACT OF THERMAL MODELS

Thermal modeling output serves as one of the dominant inputs for other waste management related models. For example, in a bedded-salt repository, corrosion of the canister wall is a primary modeling concern. The corrosion rate increases exponentially with temperature. Brine inclusions in bedded salt move toward a hot thermal source at a rate proportional to the local temperature gradient. The spent fuel retrieval option requires thermal environmental definition as an input for repository design. Some creep models for salt indicate that the creep rate is a function of the 9.5 power of temperature.[3] Clearly then, it is important that numerical modeling techniques be employed that accurately calculate the time-dependent temperature distribution.

*RRY = Reference Reactor Year, as used in NUREG-0116, is a 1000-MWe reactor operating at 80% capacity for one year.

STORAGE IN DEEP GEOLOGIC MEDIA

The concept of storage of nuclear waste in deep stable geologic media has been qualitatively considered for more than twenty years. Only during the current decade has serious effort been started in quantifying causes and effects associated with deposition of thermally and radioactively hot masses in deep geologic media. During the past three years extensive effort has been directed toward thermal modeling of repositories using finite difference and finite element techniques.[3-5] During 1978 a 3-D thermal analysis of a conceptual deep repository was begun at LLL using the code TRUMP.[6] This was one of the first known successful efforts to model 3-D time-dependent temperatures resulting from emplacement of nuclear waste.

Prior to studies conducted at LLL during the last half of 1978 it was generally thought that 2-D thermal analysis would suffice as an input source in the determination of the thermal stress field. It was assumed that an axisymmetric 2-D analysis would give accurate results near the canister and that planar 2-D analysis would give sufficiently accurate temperature data for the far-field. Essentially all of the DOE-sponsored work and most of the NRC-sponsored work prior to 1978 applied 1-D and 2-D analysis.[3-5] The results presented in the following pages show that serious error may result from relying on 2-D modeling for the canister's near-field (i.e., within a distance of several canister diameters).

PHYSICAL CHARACTERISTICS AND THERMODYNAMIC PROPERTIES OF A CONCEPTUAL WASTE REPOSITORY IN SALT

THE REPOSITORY GEOMETRY MODELED

The physical concept of a nuclear waste repository is illustrated in Fig. 1. The vertical transporter shaft serves as a feeder to several long rooms, mined in a layer of bedded salt 2000 ft (607 m) below the surface. The rooms are 18 by 18 ft (5.5 by 5.5 m) in cross section. Modeling efforts, currently in progress, will provide an understanding of causes and effects associated with the various canister emplacement options. The option studied here involves waste canisters emplaced in a series of holes drilled in the floor of each room on equal spacings of 17.32 ft (5.3 m). The distance between rooms was assumed to be 88 ft (26.8 m). Holes were assumed to be backfilled. The tops of each canister were assumed to be 10 ft (3.05 m) below the floor surface.

THERMAL CHARACTER OF THE WASTE FORM

Altenbach[6] describes a spent fuel canister,* 1 ft (0.3 m) diam by 16 ft (4.9 m), as having a thermal power of 4.61-kW 3.44-y after removal from the reactor. Reference 4 describes a solidified high level waste (SHLW) package, 1 ft (0.3 m) diam by 8 ft (2.4 m), as having a thermal power level of 3.5 kW ten-y after reprocessing. Table 1 gives thermal power decay rates for both waste forms. Emplacement of 10-y-old SHLW or 3.44 y-old spent fuel results in an initial areal thermal loading (for spacing defined above) of 100 kW/acre and 132 kW/acre, respectively, which is presently thought to approach the safe areal loading limit for geologic media such as granite and basalt.[5]

*The spent fuel canister contained 650 PWR fuel rods.

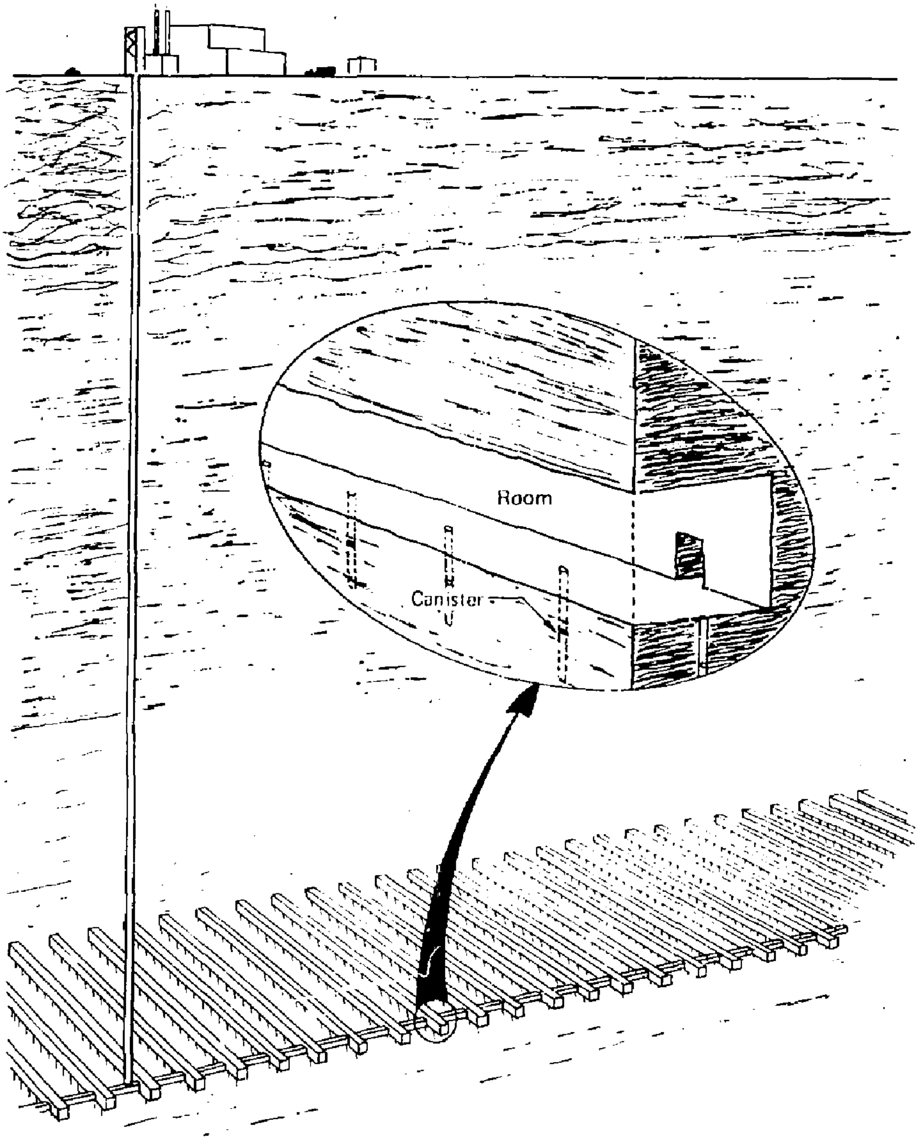

FIG. 1. Conceptual model of a nuclear high level waste repository in salt.

TABLE 1. Thermal power decay data for spent fuel[a] and SHLW.[b]

Spent Fuel		SHLW	
Time[c] y	Power, kW	Time, y	Power, kW
0.44	28.8	1.0	32.0
1.44	11.6	2.0	18.1
3.44	4.61	5.0	7.4
5.44	2.81	10.0	3.5
10.44	1.81	20.0	2.49
30.44	1.13	50.0	1.19
100.44	0.40	70.0	0.74

[a]Spent fuel consists of 650 PWR rods.[6]

[b]See reference 4.

[c]Time listed is referenced to reactor shutdown at Time = 0.

THERMODYNAMIC PROPERTIES

Thermodynamic properties of UO_2 were used in modeling the spent fuel waste form.[6] Properties of a borosilicate glass waste form were used in modeling SHLW.[4] The thermodynamic properties of salt were modeled in nonlinear fashion. A tabulation of associated thermodynamic properties is given in Table 2.

TABLE 2. Thermal modeling properties for a waste repository in salt.[4,6]

Salt:		
Density	=	135 lbm/ft^3
Specific Heat	=	0.204 Btu/lbm-^{o}F at 32^{o}F
	=	0.217 Btu/lbm-^{o}F at 212^{o}F
	=	0.222 Btu/lbm-^{o}F at 392^{o}F
	=	0.230 Btu/lbm-^{o}F at 752^{o}F
Conductivity	=	3.09 Btu/h-ft-^{o}F at 32^{o}F
	=	2.61 Btu/h-ft-^{o}F at 122^{o}F
	=	2.23 Btu/h-ft-^{o}F at 212^{o}F
	=	1.94 Btu/h-ft-^{o}F at 302^{o}F
	=	1.70 Btu/h-ft-^{o}F at 392^{o}F
	=	1.53 Btu/h-ft-^{o}F at 482^{o}F
	=	1.39 Btu/h-ft-^{o}F at 577^{o}F
	=	1.29 Btu/h-ft-^{o}F at 662^{o}F
	=	1.18 Btu/h-ft-^{o}F at 752^{o}F
Spent fuel waste:		
Density	=	655. lbm/ft^3
Specific heat	=	0.059 Btu/lbm-^{o}F
Conductivity	=	4.62 Btu/h-ft-^{o}F
SHLW:		
Density	=	200. lbm/ft^3
Heat capacity	=	0.22 Btu/lbm-^{o}F
Conductivity	=	0.58 Btu/h-ft-^{o}F
Air:		
Density	=	0.075 lbm/ft^3
Specific Heat	=	0.24 Btu/lbm-^{o}F
Conductivity	=	0.015 Btu/h-ft-^{o}F

INPUT MODELS FOR CONVECTION AND RADIATION

The long rooms above the emplaced waste were modeled as being ventilated. Average room temperature was assumed to be continuously maintained at 79°F (26°C) by a 10000 cfm/room ventilating system. The room surfaces were modeled as being cooled in accordance with Newton's Law of Cooling,[7] and the temperature-dependent convection coefficients, h, were determined from:

$h = 0.22\ (T_s - T_\infty)^{1/3}$	Floor
$h = 0.19\ (T_s - T_\infty)^{1/3}$	Vertical wall
$h = 0.068\ (T_s - T_\infty)^{1/4}$	Ceiling

where T_s is the surface temperature ($^{\circ}$F) and T_∞ is the average air temperature ($^{\circ}$F) in the ventilated room. Also, heat exchange by radiation between the room surfaces was incorporated in the 3-D TRUMP model.* Room surface properties, adapted from Gebhart,[8] are listed in Table 3.

TABLE 3. Ventilated room surface properties.

Emissivity	= 0.9
View factor (floor-to-ceiling)	= 0.41
View factor (floor-to-wall)	= 0.29
View factor (ceiling-to-wall)	= 0.29

*Incorporation of the above temperature-dependent convection coefficients and the multi-surface radiation heat exchange into the TRUMP 3-D model constitutes a relatively modest, but important, extension of the work reported by Altenbach.[6]

DEFINITION OF THE SYSTEM MODELED AND BOUNDARY CONDITIONS

In modeling both the spent fuel repository case and the SHLW case, canisters were assumed to be emplaced simultaneously in an infinitely large array according to the spacing geometry defined in an earlier section (the Repository Geometry Modeled). By imposing this condition one recognizes that a rectangular adiabatic boundary exists around each canister in the infinite array. The boundaries of any particular canister are defined by the intersecting vertical planes that pass through the mid-point spacing between the canister and its nearest neighbor. If the time period of interest is less than the first five years,* one can safely assume the geologic media temperature 500 ft (152 m) above or below the thermal source will not change during that time period due to the source. (Modeling results confirm the validity of this assumption.) Thus, a unit cell can be defined for the purpose of studying the time-dependent temperature distribution in a repository with an infinite array of waste canisters simultaneously emplaced. The unit cell is 88 by 17.32 by 1000 ft (26.8 by 5.3 by 305 m) with adiabatic boundaries on the four vertical surfaces and fixed temperatures on the top and bottom surfaces. Initial conditions on the geologic media were imposed by the geothermal gradient; the top surface was fixed at 83°F (28°C) and the bottom surface fixed at 104°F (40°C). Because of symmetry it is necessary to map only one-quarter of the complete unit cell. The quarter symmetry model is shown in Fig. 2.

*For periods of interest extending beyond five years the unit cell height should be extended to the earth's surface where convection/radiation boundary conditions are imposed; the unit cell depth should be extended to 2000 ft below the canister. The bottom boundary condition should be fixed corresponding to the natural geothermal temperature.

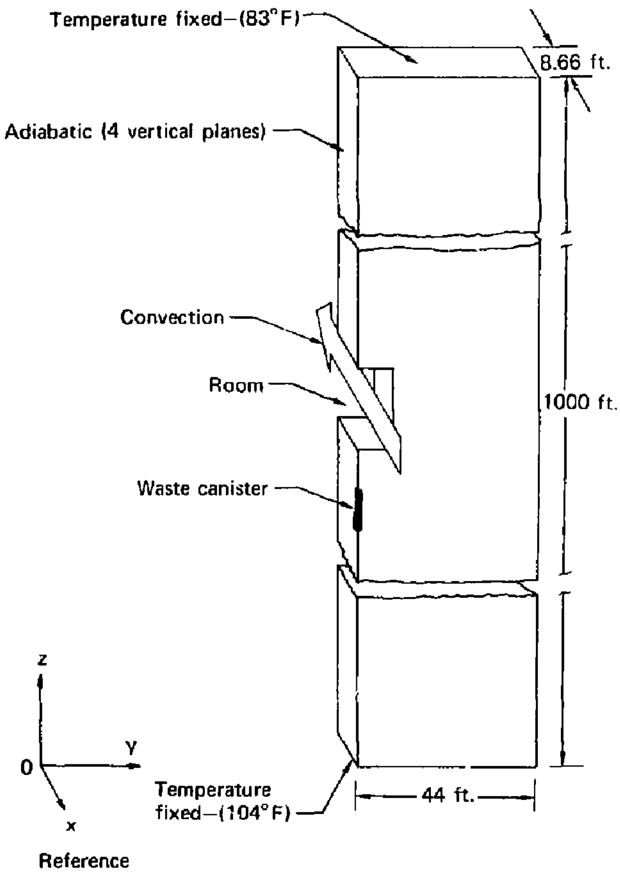

FIG. 2. Quarter-symmetry 3-D unit cell.

APPLICABILITY OF 2-D MODELING TO A NUCLEAR WASTE REPOSITORY

For reasons of practicability one always tries to define a modeling problem so that 3-D analysis can be avoided, and almost always it is possible to model a dynamic event 2-dimensionally and glean sufficiently realistic results. Reduction of the 3-D quarter-symmetry unit cell to a 2-D model can be accomplished by applying 2-D planar modeling for determining the far-field temperature distribution or applying 2-D axisymmetric modeling for determining the near-field temperature distribution. With 2-D planar modeling the X-gradients vanish (see coordinate diagram, Fig. 2) and with 2-D axisymmetric modeling the ϕ-gradients are forced to 0. Problems arise in the axisymmetric model because of the nearness to the thermal source of one adiabatic boundary relative to the distance to the other.

THE 2-D PLANAR MODEL

In the 2-D planar model X-gradients vanish when the 3-D thermal source is smeared across the entire width of a quarter-symmetry unit cell as illustrated in Fig. 3. While the total thermal power of the source does not change through this modeling process, the model heat flux near the thermal source is greatly reduced because the source is spread over a much increased area. The result is that the model produces Y-gradients near the thermal source much too low and, therefore, the model produces a near-field temperature distribution whose values are lower than those that actually occur. But since the thermal energy input is the same as it would be in the 3-D model the total energy absorbed by the geologic media in a fixed time period is also the same. For these reasons 2-D planar modeling should produce temperature distributions in the far field that are compatible with 3-D results.

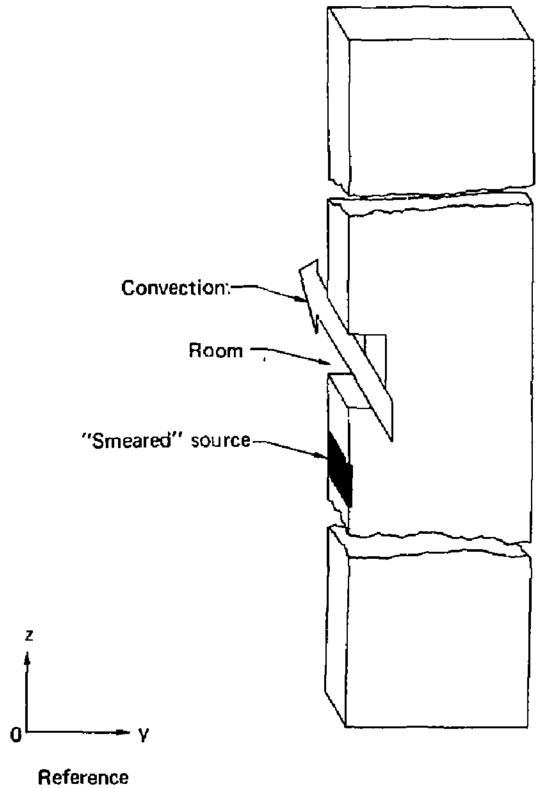

FIG. 3. Quarter-symmetry 2-D planar unit cell.

ϕ-gradients vanish in a 2-D axisymmetric model. The result, physically, is analogous to forcing the 3-D quarter-symmetry unit cell into a 2-D quarter-symmetry cylindrical shape as illustrated in Fig. 4. Considering the original basis from which the 3-D unit cell evolved (infinite array of sources activated simultaneously) one can intuitively sense the possibility of a poor fit by the axisymmetric model.

For the case where a single canister is emplaced in an infinite medium, modeling with 2-D axisymmetric would give excellent results. Also, for the case of an infinite array of canisters, better modeling results would be produced from a 2-D axisymmetric analysis if the array were more nearly square. (Note, however, the cross section of the conceptual model 3-D unit cell has an aspect ratio greater than 5.) Mining economics coupled with local geologic stability considerations are among those factors that force large cross-sectional aspect ratios.

When the 2-D axisymmetric model in Fig. 4 is used, one must decide upon a best choice for the distance, R, which is the effective distance from the center of the canister to neighboring adiabatic planes. The nearest distance to an opposing adiabatic boundary is 8.66 ft (2.6 m). The furthest distance to an opposing adiabatic boundary is 44 ft (13.4 m). The surface temperature response of the canister is greatly influenced by the proximity of an adiabatic boundary. In the real case this distance obviously varies by a factor of 5X within a 90^{0} arc centered at the canister. (See Fig. 2.) The axisymmetric model allows its user to specify only one constant-value-distance from the canister center to the adiabatic boundary. This dilemma is the source of error produced by imposing 2-D axisymmetric modeling to the unit cell.

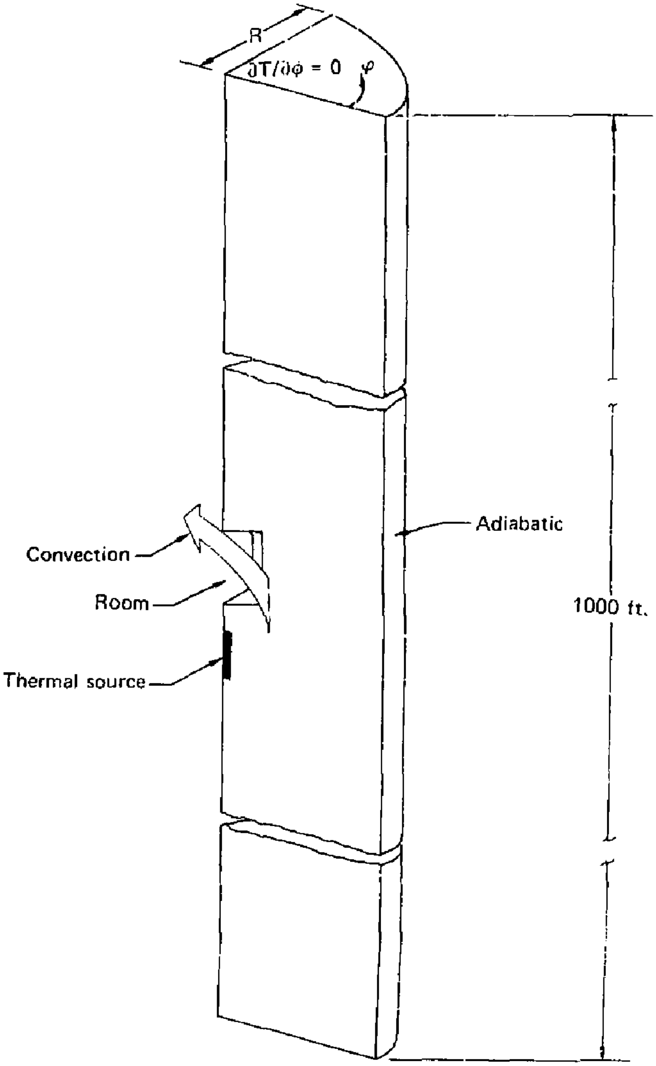

FIG. 4. Axisymmetric 2-D quarter-symmetry unit cell.

MODELING RESULTS*

Results from 3-D TRUMP modeling were used as criteria for defining the limits of applicability of 2-D modeling. Appendix A contains selected temperature response plots from 3-D analysis. ADINAT was employed for the 2-D analysis. Credibility of ADINAT-produced results was established by the extensive comparison of results from 2-D TRUMP and 2-D ADINAT in response to identical inputs. Appendix B presents some detail associated with the TRUMP vs ADINAT evaluation. The time step and mesh sensitivity of ADINAT was also evaluated. Related details appear in Appendix C.

RESULTS: 2-D Planar

A radial temperature profile for spent fuel is shown in Fig. 5. The time corresponding to this profile is five months after emplacement, which is the time at which the canister surface temperature peaks. The 3-D analysis shows that the canister surface peaks at 348°F (175°C) and the mid-pillar temperature has risen to 98°F (37°C). It is observed that 2-D model results are essentially the same as 3-D results at distances greater than one canister length† away from the thermal source; of equal importance is the fact that local temperature-peaks have the same time of occurrence in both 3-D and 2-D results.**

*Unless stated otherwise results are based on 3.44-y-old spent fuel and 10-y old SHLW.

†If one wishes to examine other analysis details which are not adressed in this section, the entire time-dependent temperature distribution input/output results are in mass storage for all 2-D and 3-D cases studied. See Appendix D for retrieval details.

**Only two lengths were modeled, 16 ft and 8 ft. It may simply be coincidental that 2-D planar fits 3-D model results at distances greater than one canister length.

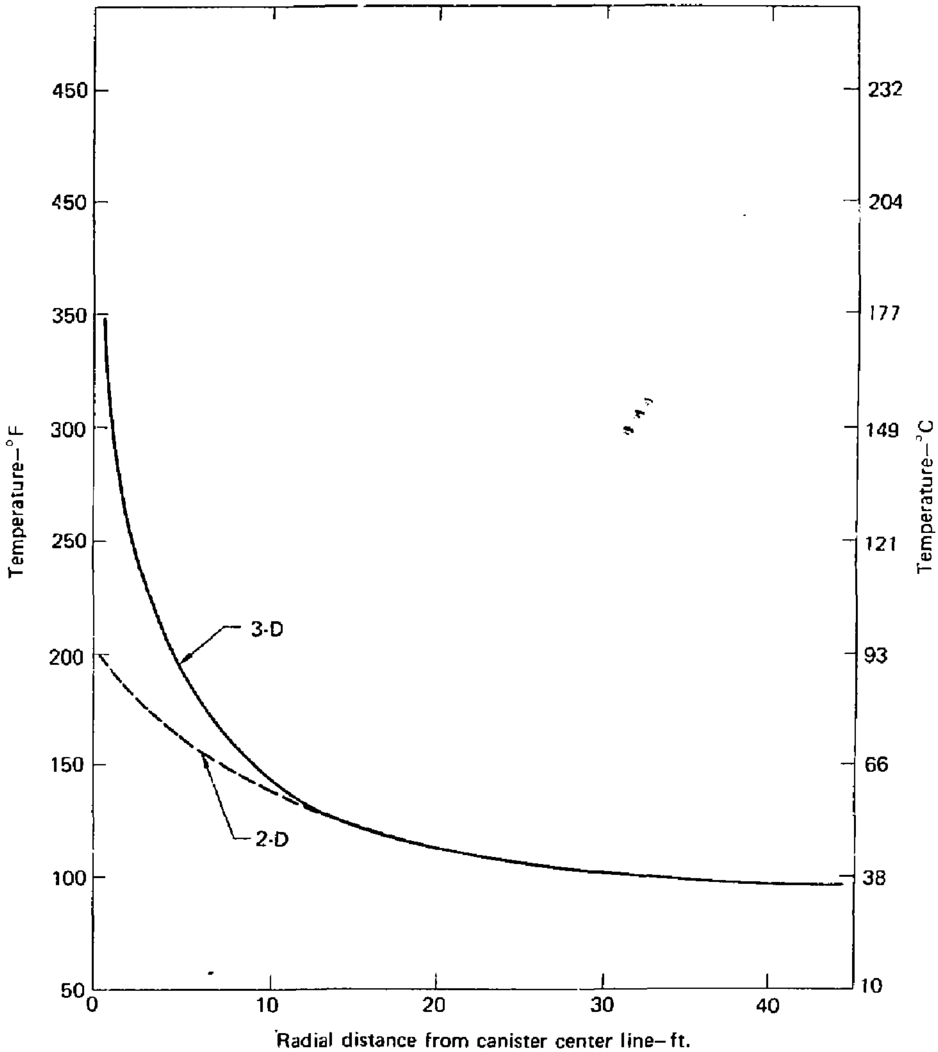

FIG. 5. Radial temperature profile for spent fuel five-months after emplacement, as determined by 2-D planar and 3-D numerical analysis.

A radial temperature profile for solidified high level waste is shown in Fig. 6. The canister surface temperature peaks five years after emplacement. (The profile in Fig. 6 corresponds to that time.) As in the case of spent fuel, agreement with 3-D results is fairly good (within 2.5°C) at distances greater than one canister length away from the thermal source. An explanation of why 2-D planar results for spent fuel have better far-field agreement than does SHLW is given in a later section (Discussion of Results).

RESULTS: 2-D AXISYMMETRIC

Results for three 2-D axisymmetric model cases are superimposed over the 3-D profile for spent fuel in Fig. 7. The distance, R, from source-to-adiabatic boundary is the only difference in the three cases. The plots illustrate only the profile-sensitivity to radius. The temperature time histories are also quite sensitive to the radius. It should be emphasized that the axisymmetric profiles in Fig. 7 are plotted for a time of five months after emplacement, corresponding to occurrence of actual peak surface temperature. Except for the 22-ft (6.7 m) radius, the model results predict the time and magnitude of peak surface temperature to be very different from the 3-D baseline results. Table 4 summarizes these related details.

TABLE 4. Axisymmetric peak surface temperatures and time of occurrence.[a]

Radius ft	Peak surface temp., °F	Time of peak after emplacement, months
9.0 (2.74 m)	493.3 (526.3°C)	15
12.0 (3.66 m)	369.3 (187.4°C)	12
22.0 (6.70 m)	287.6 (142.0°C)	5

[a] 3-D analysis shows peak surface temperature of 348°F (176°C) to occur five months after emplacement.

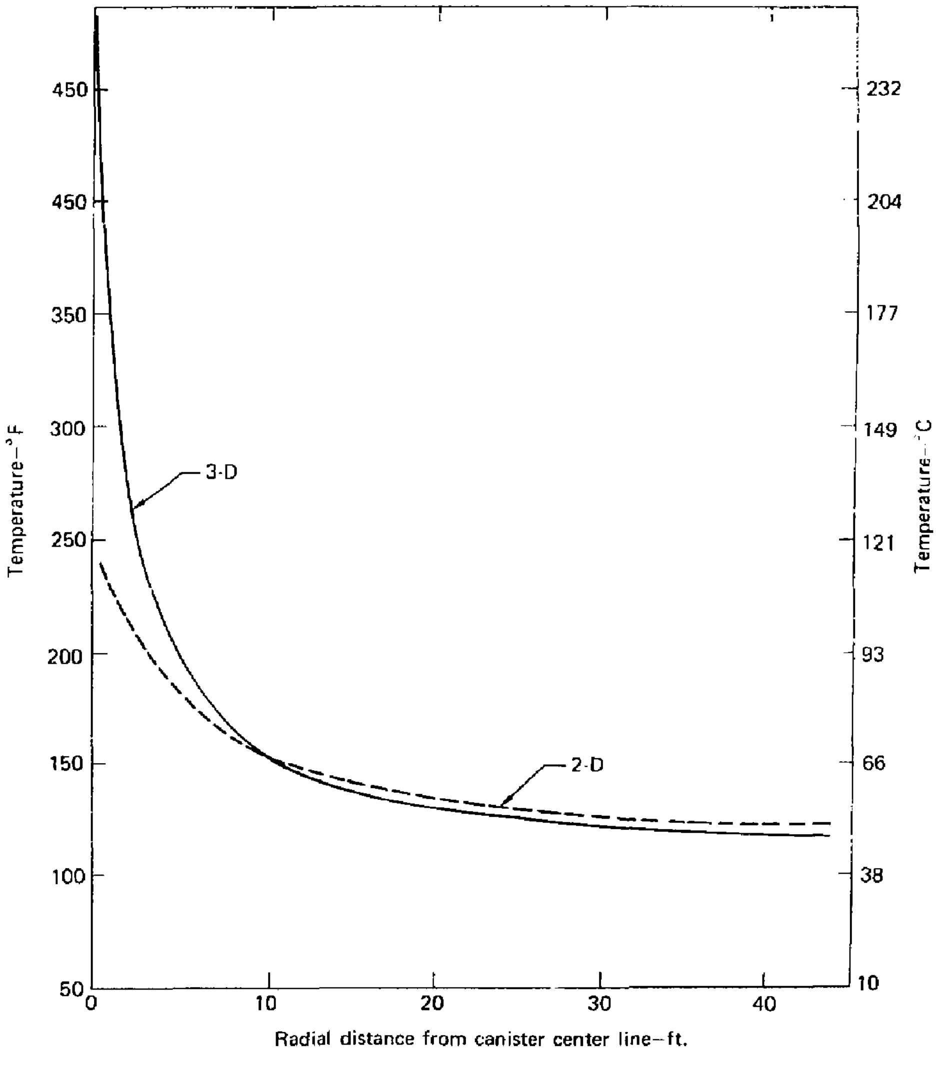

FIG. 6. Radial temperature profile for SHLW five years after emplacement, as determined by 2-D planar and 3-D numerical analysis.

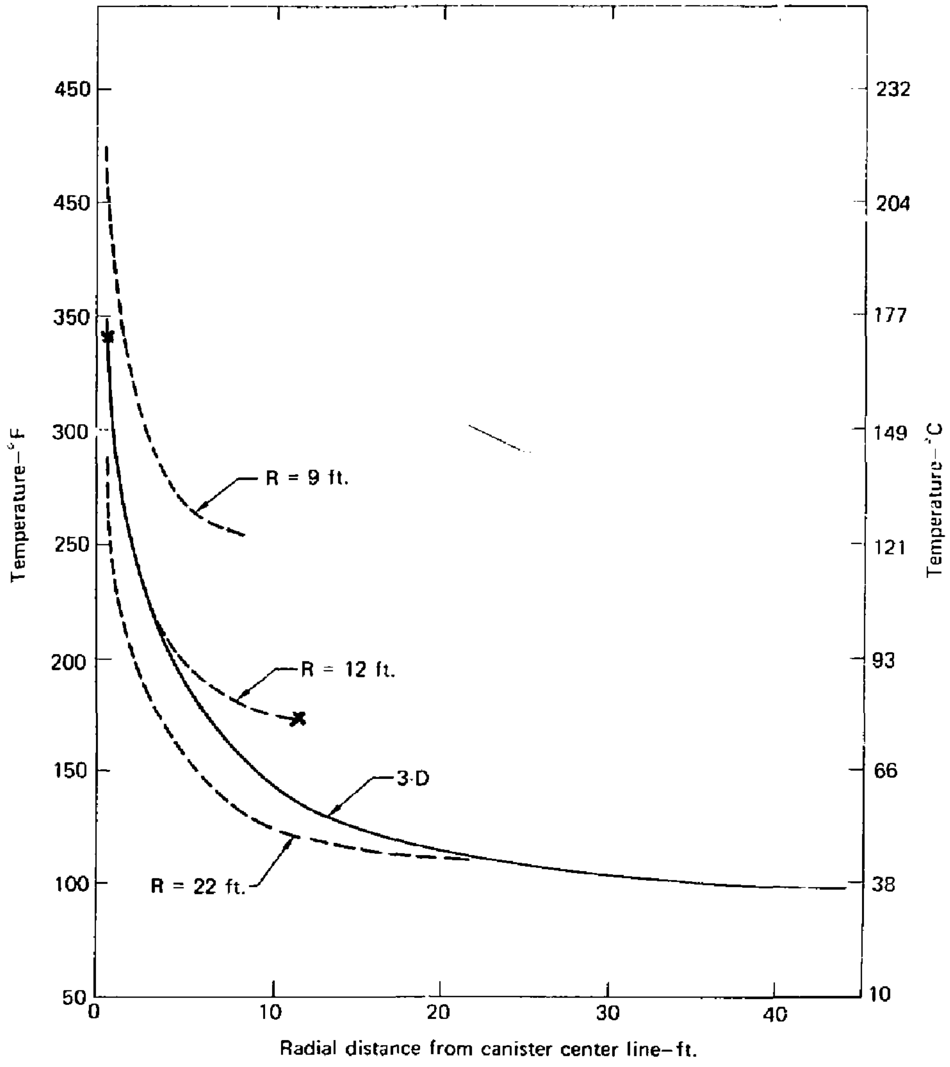

FIG. 7. Comparison of 2-D axisymmetric with 3-D results for a spent fuel repository.

These results point to the inability of 2-D axisymmetric modeling to produce near-field temperature distributions which have correctness of both magnitude and timing. That is, if the radius is adjusted so that peak temperatures are correct, then the time of peaks are incorrect. Both time and magnitude must be tightly coupled, especially for salt repositories, if thermal stress models are to yield credible results.

DISCUSSION OF RESULTS

Results from 2-D thermal modeling provide useful inputs for other repository predictive models if their resultant time-dependent temperature distributions closely match that of 3-D models.

Axisymmetric 2-D

The 22-ft (6.7-m) radius best matches 3-D model results, but its agreement is probably not sufficiently accurate to be used as an input for other salt repository models, such as numerical thermal stress analysis. The basis for this concern is the strong temperature- and time-dependent nature of creep rate in salt. The 22-ft (6.7-m) radius is the only one of the three considered above that has an a priori logical basis for its choice. It is the radius which prescribes a 2-D unit cell mass equal to the mass of the 3-D unit cell. Because of the mass equality one should expect the average temperature response of 2-D and 3-D models to be the same. While the averaged temperature response of the two models will be the same, the 2-D axisymmetric model, by definition, cannot reflect the ϕ-related time-dependent distortions in temperature due to the two opposing adiabatic boundaries having widely-differing distances from the thermal source.

Planar 2-D: Definition of Far-Field

Far-field is defined as that region of the unit cell that can be accurately modeled with 2-D planar. Thus, the geometric far-field region is a function of the size and shape of the waste form, as deduced by comparing Figs. 5 and 6. Results from the two waste form geometries studied indicate the far-field is that region of a unit cell which is greater than one canister length away from the canister surface. The above definition may not be valid for waste form geometries or repository concepts that vary greatly from those defined in an earlier section (Physical Characteristics and Thermodynamic Properties of a Conceptual Waste Repository in Salt).

Planar 2-D: Nonlinear Salt Properties

Referring again to Fig. 6, the agreement with 3-D results in the far-field is not as good for SHLW as it is with spent fuel. The nonlinear properties of salt (conductivity) causes this apparent modeling defect. Note the strong nonlinearity of thermal conductivity of salt in Table 2. Relative to other geologic materials salt is a good thermal conductor. Nevertheless, it serves as a resistance to heat flow from the canister. Higher temperatures in the canister near-field cause a substantial increase in the resistance to heat flow. Since the 2-D planar analysis does not yield those higher near-field temperatures, the model naturally does not build the same resistive blanket around the canister near-field that the 3-D model does. Note that this effect is amplified in a SHLW repository by two factors. The actual 3-D near-field temperature is higher than spent fuel and the time lapse between waste emplacement and occurreance of peak temperature is 12 times greater for SHLW than for spent fuel. The greater SHLW temperature differential results in a greater difference in near-field resistive blankets. The longer time period allows a greater heat-flow-integration-time which reflects temperatures in the far-field that are erroneously high.

General Comments--2-D Modeling

When one employs 2-D planar modeling for SHLW, the nonlinear conductivity model should be scaled up for the near-field temperature range so that improved far-field time-dependent temperature distributions can be produced. To define the scaling model properly, a more extensive analytical effort is needed. It is conceivable that one could derive a scaling transfer function which could transform the nonlinear conductivity set into an artificial set whose use with 2-D axisymmetric models would yield useful near-field results; it is questionable whether such effort is justified in view of LLL's 3-D stress analysis capability with ADINA. For analysis of geologic media other than salt, 2-D axisymmetric modeling may give sufficiently accurate results. With salt, however, many of the performance-related events that must be modeled have an inordinately strong dependence on the integrated local effects due to the magnitude of temperature, time, and temperature gradients. The brine migration velocity, for example, is directly proportional to the local temperature gradient,[9] and the creep rate varies in proportion to $T^{9.5}$, according to Talbot.[3]

CONCLUSIONS

By comparing results from 2-D and 3-D thermal modeling of a high level waste repository, certain conclusions can be deduced regarding the applicability of 2-D techniques. They are summarized below:

1. Two-dimensional planar modeling of a spent fuel repository is applicable to the far-field of the unit cell. For the two wasteform geometries modeled, the far-field is that geometric region of the unit cell which is greater than one canister length away from the surface of the thermal source.

2. Two-dimensional planar modeling of a SHLW is applicable to the far-field region. Improved modeling results are possible through scaling of the nonlinear material conductivity set for the near-field temperature range.

3. Axisymmetric 2-D modeling is not directly applicable to thermal modeling of any portion of a high level waste repository in salt. It is however, conceivable that a scaling transformation of the nonlinear conductivity set could render axisymmetric model results useful.

4. The highly nonlinear nature of salt material properties complicates the applicability of 2-D thermal modeling of a salt repository. A simiiar sort of complication should be anticipated in stress and creep flow modeling.

5. With reference to Appendices B and C, results for far-field 2-D thermal modeling from TRUMP and ADINAT agree within one percent. ADINAT is relatively sensitive to mesh aspect ratio. Although stability of ADINAT appears to be insensitive to magnitude of the time step, solution convergence requires a minimum of ten cycles of the time step.

APPENDIX A

TEMPERATURE RESPONSE

For the purpose of gaining perspective, it is helpful to consider the large variation in time of occurrence of temperature peaks within the unit cell. Figure A.1 shows the temperature response at three different points located on a line extending radially from a spent fuel canister to the center of the salt pillar dividing two adjacent rooms. Figure A.2 shows a similar set of response curves at the same locations in a SHLW repository. Plots in both figures are from 3-D TRUMP modeling. Because the effective time constant for SHLW is greater than spent fuel a two-year time frame is used to display the spent fuel response and a fifty-year time frame displays the SHLW response. When one qualitatively considers the combined effect of creep and thermal expansion on the integrity of the waste form, it becomes clear how important the time aspect of the temperature field is. Creep occurs at all temperatures, but is accelerated at higher temperatures while local thermal expansion occurs when the time-rate-of-change of temperature is positive. The two mechanisms combine in complex fashion to provide the source for the dynamic component of stress. Hence, thermal modeling that becomes the input for stress models must accurately capture both temperature magnitude and time-dependence in the entire geometric field.

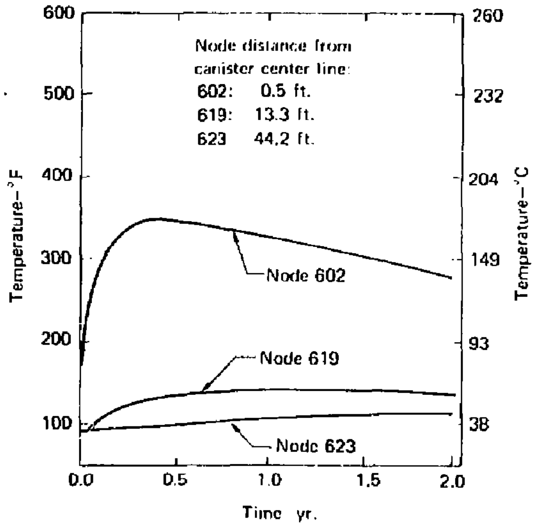

FIG. A.1. Temperature response of selected nodes in the salt at radial points in the mid-plane of the spent fuel canister.

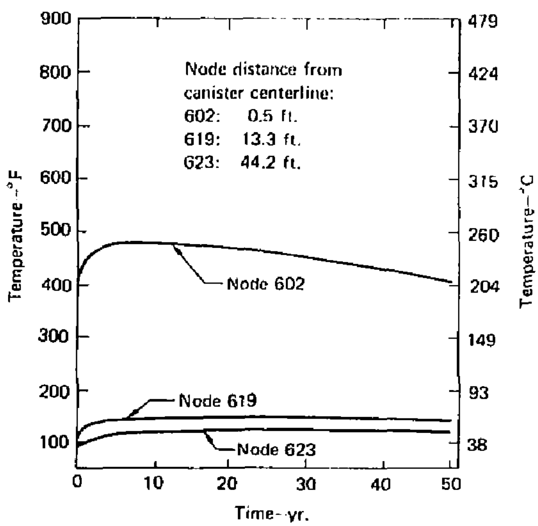

FIG. A.2. Temperature response of selected nodes in the salt at radial points in the mid-plane of the SHLW canister.

APPENDIX B

COMPARISON OF TRUMP AND ADINAT

TRUMP is a finite difference nonlinear analysis thermal code developed at LLL by A. Edwards[10] which has a broad history of successful use. ADINAT[11] is a finite element nonlinear analysis thermal code developed at MIT which is relatively new and consequently has had limited exposure to LLL users. Both codes have 3-D capability. ADINAT has a companion stress code, ADINA; the two codes use compatible element and nodal point specifications and, therefore, are attractive choices for performing thermal/thermal stress analysis.

A study was conducted in which the performance of ADINAT was investigated. A 2-D planar analysis was made in the spring of 1978 using TRUMP.* The model input parameters were duplicated in a suitable format and used in ADINAT. Agreement of the two codes was found to be remarkably good in the far-field as shown in Fig. B.1.

---

*T. J. Altenbach, LLL, developed a 2-D mesh and executed a TRUMP computer run. A constant convection coefficient of 0.6 Btu/h-ft-^{o}F was specified for the ventilated room. Radiation from room surfaces was ignored. The thermal source had an initial power of 5 kW and a decay rate equal to that of SHLW.

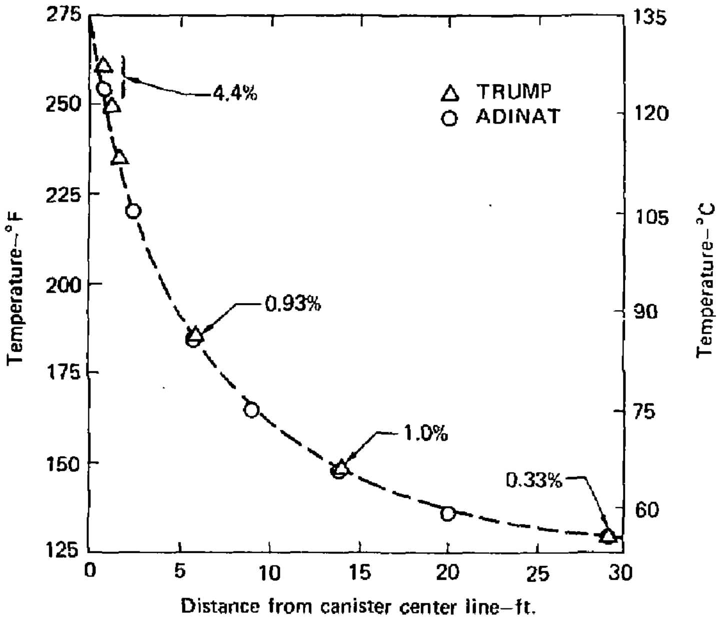

FIG. 8.1. Mid-plane radial temperature profile comparing ADINAT with TRUMP. Time after emplacement is three years and the source power at emplacement was 5 kW (SHLW).

APPENDIX C

ELEMENT ASPECT RATIO AND TIME-STEP SENSITIVITY OF ADINAT

Results of a 2-D comparison of TRUMP and ADINAT show ADINAT to be more sensitive to mesh aspect ratio than TRUMP. ADINAT is extremely stable in response to time-step variation; TRUMP, however, is quite sensitive to time-step magnitude.

SENSITIVITY OF ELEMENT ASPECT RATIO

Figures C.1 and C.2 illustrate the effect of the mesh aspect ratio on ADINAT-produced temperature response. Mesh-1 and Mesh-2, inset in Fig. C.1, are both finite element grids used in ADINAT. They differ only by the vertical line of Mesh-2 that diminishes the aspect ratio of the mid-section elements. That simple addition causes a significant change in the calculated temperature response. The location of Node-93, marked on the two grids, is 5.25 ft (1.6 m) for the canister surface. Similar differences are notable at all nodal points. Figure C.2 illustrates the effect of further mesh refinements. The inset marked Mesh-3 adds another vertical line and additional grid adjustments to produce a more favorable element aspect ratio. The top curve (Mesh-3) is essentially identical to the response produced by TRUMP.

Rigorous quantification of output sensitivity to mesh aspect ratio may be an impossible task. The mesh sensitivity to calculated accuracy response is affected by mechanisms other than geometry. Transient characteristics and gradient magnitude will impact on mesh sensitivity. It will be necessary for any new ADINAT finite element mesh to be carefully varied to determine whether the grid is fine enough to produce a stable temperature response. A mesh that is too coarsely gridded causes an increase in apparent heat capacitance,* which results in a calculated temperature field with decreased magnitude.

*The calculated results project characteristics which would be expected if the heat capacitance were larger than that actually input. A larger "apparent heat capacity" is manifested in lower field temperature and later peaking.

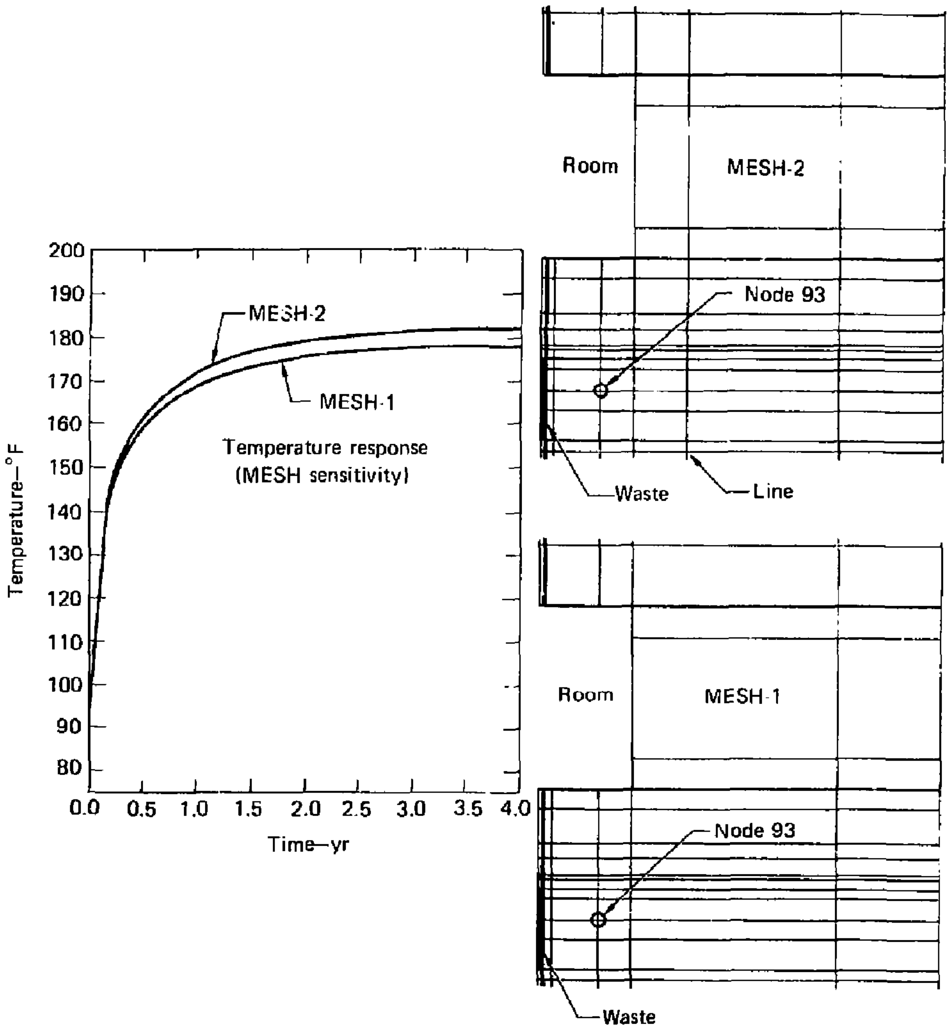

FIG. C.1. Temperature response of Node-93 (5.25 ft from canister surface) for two similar meshes from ADINAT.

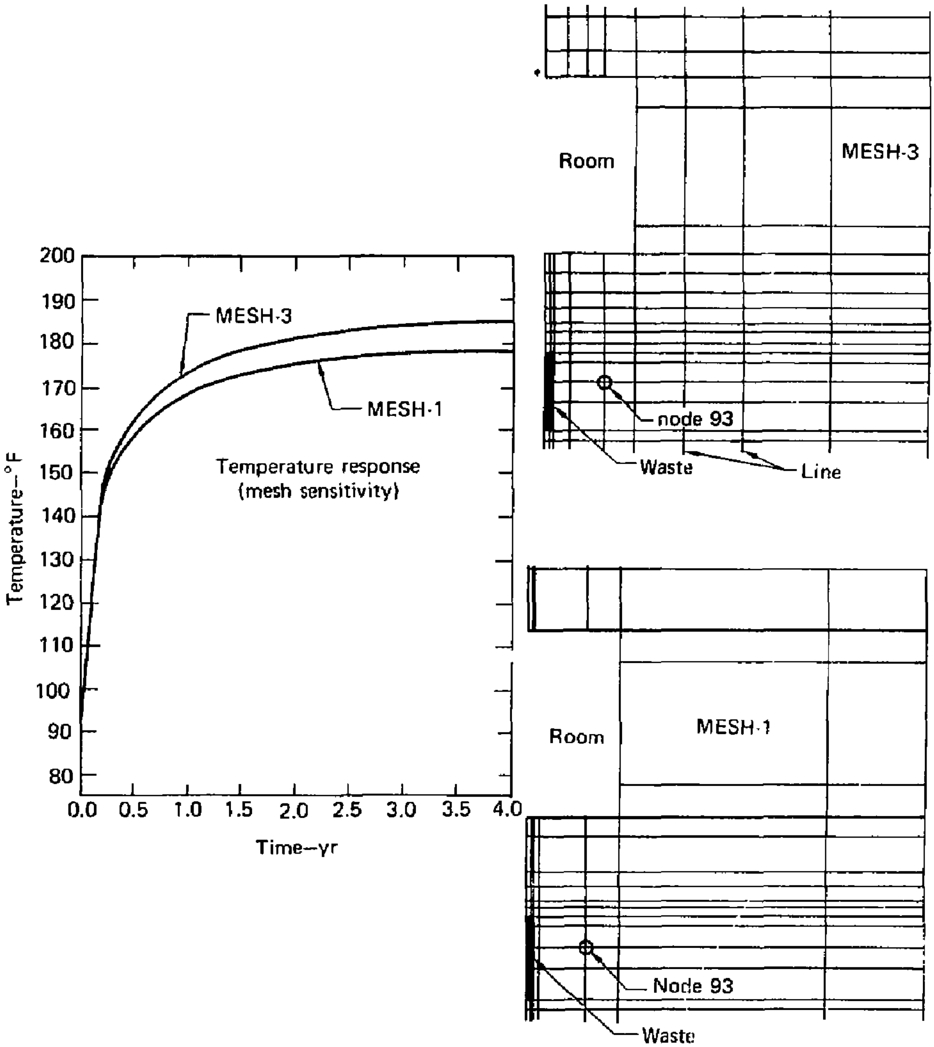

FIG. C.2. Temperature response of Node-93 (5.25 ft from canister surface) for two different meshes.

TIME-STEP SENSITIVITY

ADINAT was found to be stable for time-steps ranging from 1 second to 5 years for 2-D analysis. A series of computer runs was made using successively increasing time-step values. While stability is not a problem, it was observed that a minimum of 10 time-steps are needed for the ADINAT solution to converge to the correct solution; this is illustrated in Fig. C.3. The solid line is the correct temperature response on Node-93. (See Fig. C.2 for location.) The dashed line is the response for a time-step of 1 year. Both curves were produced by ADINAT; the solid curve was produced using a time-step of 360 hours. The convergence trend is seen in the two curves. They will converge at the 10-year point in time (ten time-steps of the dashed response). Thus, if one chooses a time-step of 1 year, the output data is valid for the time period following the tenth year.

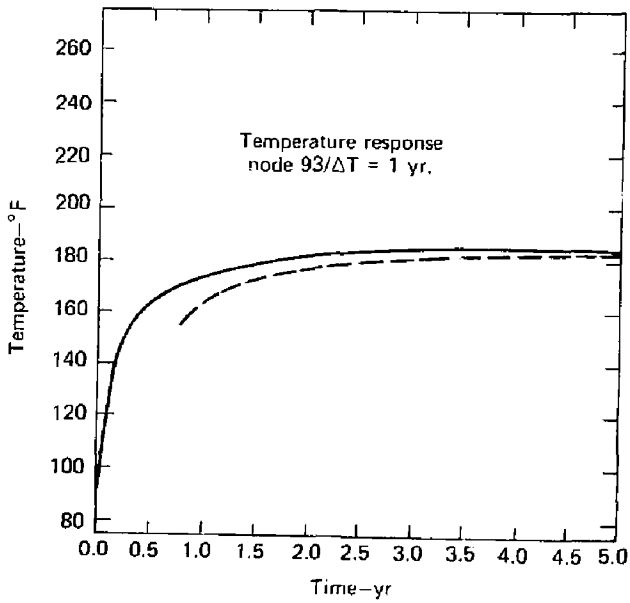

FIG. C.3. Convergence of Node-93 correct temperature response and response for a 1-year time step.

APPENDIX D

MASS STORAGE OF NUMERICAL RESULTS

To enable investigators to examine details not specifically discussed in the text and to allow investigators to extend more easily the work presented herein, all of the important inputs and outputs of the numerical analysis effort was XPORTed to mass storage. The directories and files of interest may be accessed through the following user number:

User No: 203525

The directories and files of interest are defined below:

DIRECTORY: .SPENTAXIS

This directory contains all of the ADINAT input and output files pertaining to axisymmetric 2-D numerical modeling of a spent fuel repository. File names and descriptions follow.

INAX-R12 -- Input* file, ADINAT, for radius = 12 ft
INAX-R22 -- Input file, ADINAT, for radius = 22 ft
INAX-R9 -- Input file, ADINAT, for radius = 9 ft

PSLOPEA42 -- Output* file, ADINAT, for radius = 12 ft
PSLOPEA40 -- Output file, ADINAT, for radius = 22 ft
PSLOPEA41 -- Output file, ADINAT, for radius = 9 ft

*The input files specify element configurations, nodal point locations, boundary conditions, initial conditions, physical properties, etc.; the output files are the calculated time-dependent temperature responses corresponding to each input set.

DIRECTORY: .SPENTPLAN

This directory contains the ADINAT input file and corresponding output file for 2-D planar numerical modeling of a spent fuel repository. Files of particular interest are:

INPLAN37 -- Input file, ADINAT, 2-D planar
PSLOPEA37 -- Output file, ADINAT, 2-D planar

DIRECTORY: CASE9B

This directory contains the TRUMP input file and corresponding output files for 3-D numerical modeling of a spent fuel waste repository. The input file incorporates temperature dependent convection from all walls of the ventilated room. It also incorporates radiation exchange between the vertical walls, floor, and ceiling. Files of interest are:

BOA9AINB -- Input file, TRUMP, 3-D spent fuel
CASE9BRUNA -- Output file, temperature distribution
CASE9BRUNB -- Output file, temperature distribution
DTRUMPX1 -- Selected set of temperature responses (DD80)

DIRECTORY: .CASE9C

The input file is the same as that for CASE 9B except radiation exchange between ventilated room surfaces was not incorporated and convection from room surfaces was modeled with a constant convection coefficient of 0.4 Btu/h-ft^2-^{o}F. Files of interest are:

BOA9AINC -- Input file, TRUMP, 3D spent fuel
CASE9CRUN1 -- Output file, temperature distribution
DTRUMPX1 -- Selected set of temperature responses (DD80)

DIRECTORY: .CASE8

This directory contains SHLW inputs and outputs for 3-D TRUMP numerical modeling. The input file incorporates temperature dependent convection from all walls of the ventilated room. It also incorporates radiation exchange between the vertical walls, floor, and ceiling. Files of interest are:

BOA8AIN -- Input file, TRUMP, 3-D SHLW
CASE8RUN1A -- Output file, temperature distribution
CASE8RUN1B -- Output file, temperature distribution
DTRUMPX1 -- Selected set of temperature responses (DD80 files)

DIRECTORY: .CASE10

The input file is the same as that for CASE8 except radiation exchange between ventilated room surfaces was not incorporated and convection from room surfaces was modeled with a constant convection coefficient of 0.4 Btu/h-ft^2-^{o}F.

BOA10AIN -- Input file, TRUMP, 3-D SHLW
CASE10RUN1 -- Output file, temperature distribuion
DTRUMPX1 -- Selected set of temperature responses (DD80 files)
DTRUMPX2 -- Selected set of temperature responses (DD80 files)

DIRECTORY: .SHLW2D

This directory contains the ADINAT input file and corresponding output file for 2-D planar numerical modeling of a SHLW repository. Files of particular interest are:

INSHLW -- Input file, ADINAT, 2-D planar
PSLOPEA35 -- Output file, ADINAT, 2-D planar

ACCESSING A FILE

To access any file referenced above (for example, BOA10AIN), follow this procedure:

1. Log-on to the 7600 system with user number 203525.
2. Call XPORT:

```
XPORT / t v
.RDS .CASE10:BOA10AIN
```

REFERENCES

1. R. A. Heckman and T. Holdsworth, Determination of Performance for Solidified High Level Waste, A Preliminary Draft Report, Lawrence Livermore Laboratory, Livermore, CA, submitted to W. Hewitt of U.S. Nuclear Regulatory Commission (1978).
2. Nuclear News, 21 (10) (1978).
3. J. Byrne, Preliminary Report on Rock Mechanics Design Criteria for Nuclear Waste Repository in Salt: Very Near Field Effects During Retrievability Period, Golder Associates, Kirkland, WA, V78354 (1978).
4. D. Ensminger, M. Hough and S. Oston, Pre-Sealing Risk Analysis, A Report Prepared for Lawrence Livermore Laboratory, Livermore, CA, by The Analytic Science Corporation (TASC), September 30, 1978.
5. Dames & Moore, Inc., Thermomechanical Stress Analysis and Thermal Loading Guidelines, TM-36/20, DOE contract W-7405-Eng-26 (1978).
6. T. J. Altenbach, Interim Report on Nuclear Waste Depository Thermal Analysis, Lawrence Livermore Laboratory, Livermore, CA, UCID-17865 (1978).
7. J. P. Holman, Heat Transfer, 3rd Edition, McGraw-Hill Book Co., New York (1972).
8. B. Gebhart, Heat Transfer, 2nd Edition, McGraw-Hill Book Co., New York (1971).
9. E. Gaffney, Brine Migration, Pacifica Technology Report PT-U78-0242, August 11, 1978.
10. A. Edwards, TRUMP: A Computer Program for Transient and Steady-State Temperature Distributions in Multidimensional Systems, Lawrence Livermore Laboratory, Livermore, CA, UCRL-14754, Rev. 3 (1972).
11. K. Bathe, ADINAT: A Finite Element Program for Automatic Dynamic Incremental Nonlinear Analysis of Temperatures, Massachusetts Institute of Technology, Cambridge, MA. Report 82448-5 (1978).

EB/nll